

Amyloid

The Journal of Protein Folding Disorders

ISSN: (Print) (Online) Journal homepage: <https://www.tandfonline.com/loi/iamy20>

Enhanced detection of ATTR amyloid using a nanofibril-based assay

M. Mahafuzur Rahman, Benjamin Schmuck, Henrik Hansson, Torleif Härd, Gunilla T. Westermark & Mats Sandgren

To cite this article: M. Mahafuzur Rahman, Benjamin Schmuck, Henrik Hansson, Torleif Härd, Gunilla T. Westermark & Mats Sandgren (2021) Enhanced detection of ATTR amyloid using a nanofibril-based assay, *Amyloid*, 28:3, 158-167, DOI: [10.1080/13506129.2021.1886072](https://doi.org/10.1080/13506129.2021.1886072)

To link to this article: <https://doi.org/10.1080/13506129.2021.1886072>



© 2021 The Author(s). Published by Informa UK Limited, trading as Taylor & Francis Group.



Published online: 13 Feb 2021.



Submit your article to this journal [↗](#)



Article views: 676



View related articles [↗](#)



View Crossmark data [↗](#)

Enhanced detection of ATTR amyloid using a nanofibril-based assay

M. Mahafuzur Rahman^{a*} , Benjamin Schmuck^a , Henrik Hansson^a , Torleif Härd^a , Gunilla T. Westermark^b  and Mats Sandgren^a 

^aDepartment of Molecular Sciences, Swedish University of Agricultural Sciences (SLU), Uppsala BioCenter, Uppsala, Sweden; ^bDepartment of Medical Cell Biology, Uppsala University, Uppsala, Sweden

ABSTRACT

More than 30 proteins and peptides have been found to form amyloid fibrils in human diseases. Fibrils formed by transthyretin (TTR) are associated with ATTR amyloidosis, affecting many vital organs, including the heart and peripheral nervous system. Congo red staining is the gold standard method for detection of amyloid deposits in tissue. However, Congo red staining and amyloid typing methods such as immunofluorescence labelling are limited to relatively large deposits. Detection of small ATTR deposits present at an early stage of the disease could enable timely treatment and prevent severe tissue damage. In this study, we developed an enhanced ATTR amyloid detection method that uses functionalised protein nanofibrils. Using this method, we achieved sensitive detection of monomeric TTR in a microplate immunoassay and immunofluorescence labelling of *ex vivo* tissue from two patients containing ATTR aggregates. The system's utility was confirmed on sections from a patient with AA amyloidosis and liver sections from inflamed mouse. These results suggest that the detection system constitutes important new technology for highly sensitive detection of microscopic amounts of ATTR amyloid deposited in tissue.

Abbreviations: Ab-bNF: antibody-binding nanofibril; AA-bNF: Ab-bNF loaded with AA antibodies; TTR-bNF: Ab-bNF loaded with TTR antibodies; ATTR: amyloid transthyretin; AFM: atomic force microscopy; FB: fibrillation buffer; GAR-Alexa 488/647: goat anti-rabbit antibody conjugated with Alexa Fluor 488 or 647; SAA: serum amyloid A; TTR: transthyretin

ARTICLE HISTORY

Received 15 July 2020
Revised 27 January 2021
Accepted 2 February 2021

KEYWORDS

ATTR amyloid; AA amyloid; enhanced detection; functional protein nanofibril; immunoassay

Introduction

A broad range of human diseases arise from protein aggregation and subsequent amyloid deposition in different organs [1]. One such condition is transthyretin amyloidosis (ATTR), a systemic amyloid disease associated with deposition of transthyretin (TTR). TTR is a homotetrameric protein with molecular mass 55 kDa that natively functions as a transporter for thyroxine and retinol in the blood plasma and cerebrospinal fluid [2]. Mutations in TTR can lead to destabilisation of the tetramer, which increases the aggregation propensity and thus promotes amyloid accumulation in several different tissues, e.g. peripheral nerves, heart, eyes, and kidney [3]. Additionally, wild type (wt)-TTR can dissociate and aggregate into amyloid, which is a process that may occur with aging [4,5]. AA-amyloidosis is a second form of systemic amyloidosis that develops when protein AA, composed of N-terminal fragments of the acute phase protein serum amyloid A (SAA) deposit in peripheral organs, e.g. the spleen, liver, kidney, and the vascular tree (reviewed in [6]). AA amyloidosis occurs as a comorbidity to chronic inflammatory conditions, e.g. tuberculosis and

rheumatoid arthritis, and in recent times, the condition has been linked to obesity [7].

Congo red staining combined with polarisation microscopy is the standard technique for diagnosis of systemic amyloidosis in biopsies. Identification of amyloid precursor protein is then performed by immunohistochemistry, western blot, or mass spectrometry. The treatment options for amyloidosis are rapidly expanding, and especially research on ATTR amyloidosis has resulted in different treatment strategies. Liver transplantation, the previous first-line treatment [8], is being replaced by recently developed promising TTR kinetic stabiliser drugs, such as diflunisal [9] and tafamidis [10], and by genetic therapies, e.g. patisiran [11]. However, to achieve the greatest benefits from these advanced drugs, detection of a small amount of ATTR deposits in the tissue during the early course of disease is essential. Since tissue damage already inflicted by ATTR amyloidosis is irreparable, immediate treatment can limit tissue damage and retain the patient's quality of life.

Congo red staining to confirm the presence of amyloid is applied on a routine basis, but has obvious limitations, such as limited sensitivity [12]. Amyloid deposits are unevenly

CONTACT Mats Sandgren  mats.sandgren@slu.se  Department of Molecular Sciences, Swedish University of Agricultural Sciences (SLU), Uppsala BioCenter, Box 7015, SE-750 07 Uppsala, Sweden

*Current address: Department of Chemistry, KTH Royal Institute of Technology, SE-100 44 Stockholm, Sweden

© 2021 The Author(s). Published by Informa UK Limited, trading as Taylor & Francis Group.
This is an Open Access article distributed under the terms of the Creative Commons Attribution-NonCommercial-NoDerivatives License (<http://creativecommons.org/licenses/by-nc-nd/4.0/>), which permits non-commercial re-use, distribution, and reproduction in any medium, provided the original work is properly cited, and is not altered, transformed, or built upon in any way.

distributed and patients in an early stage of the disease have minuscule deposits; therefore, it is necessary to obtain biopsies of adequate size. Congo red staining has an increased risk of producing false negative results in these cases [13]. Fluorescent dye probes have been developed to improve the sensitivity of detection, enabling enhanced detection of amyloid aggregates as a complementary approach to Congo red dye [14–16]. One such probe, the heptamer formyl thiophene acetic acid (h-FTAA), indicated that this dye is more sensitive [17,18], although less specific [19], than Congo red. In addition to the development of new dyes, many laboratories are attempting to amplify tissue existing ATTR by exploiting the amyloid seeding approach. However, this strategy may not be feasible, because monomer addition in the case of TTR is energetically favourable and nuclei formation is not required for efficient aggregation [20].

Here, we introduce a protein nanofibril-based assay with high sensitivity for detection of ATTR in biopsies from patients with amyloidosis. Our assay relies on recently developed antibody-binding nanofibrils (Ab-bNF), which have 20-fold higher binding capacity than Protein A-Sepharose (GE Healthcare) [21]. The translation release factor Sup35(1-61) (abbreviated Sup35) from *Saccharomyces cerevisiae* serves as a scaffold for the Ab-bNF. Sup35 is an amyloid-forming protein and Ab-bNF are assembled by co-fibrillation of Sup35 with Sup35-ZZ, a genetic hybrid of Sup35 and the antibody-binding Z-domain dimer (ZZ). This fibrillation protocol leads to the exposure of ZZ on the

surface of the Sup35 fibrils, allowing for the primary antibodies to bind (Figure 1). Only a few primary antibodies present on the Ab-bNF are expected to participate in antigen binding, while the remaining antibodies act as secondary antibody binding sites. In addition to signal amplification, we also expect increased sensitivity based on cooperative antigen binding of the tightly packed antibodies immobilised along the Ab-bNF.

Methods

Proteins production

An engineered monomeric TTR (one subunit, henceforth called M-TTR) was recombinantly expressed and purified as described elsewhere [22,23]. *Escherichia coli* BL21star (DE3) cells were transformed with the bacterial expression vector pMMH α containing genes for M-TTR. The transformed cells were grown at 37°C in Lysogeny Broth (LB) medium containing 150 μ g/mL ampicillin, with shaking at 180 rpm until the optical density at 600 nm reached 0.8. Expression of M-TTR protein was induced by the addition of isopropyl β -d-1-thiogalactopyranoside (IPTG; Formedium, Hunstanton, UK) to a final concentration of 2 mM. Following induction, the temperature was lowered to 17°C, and the cells were allowed to grow overnight. The cells were harvested by centrifugation at 4,500 rpm for 20 min at 4°C in a Sorvall LYNX 6000 (Thermo Scientific,

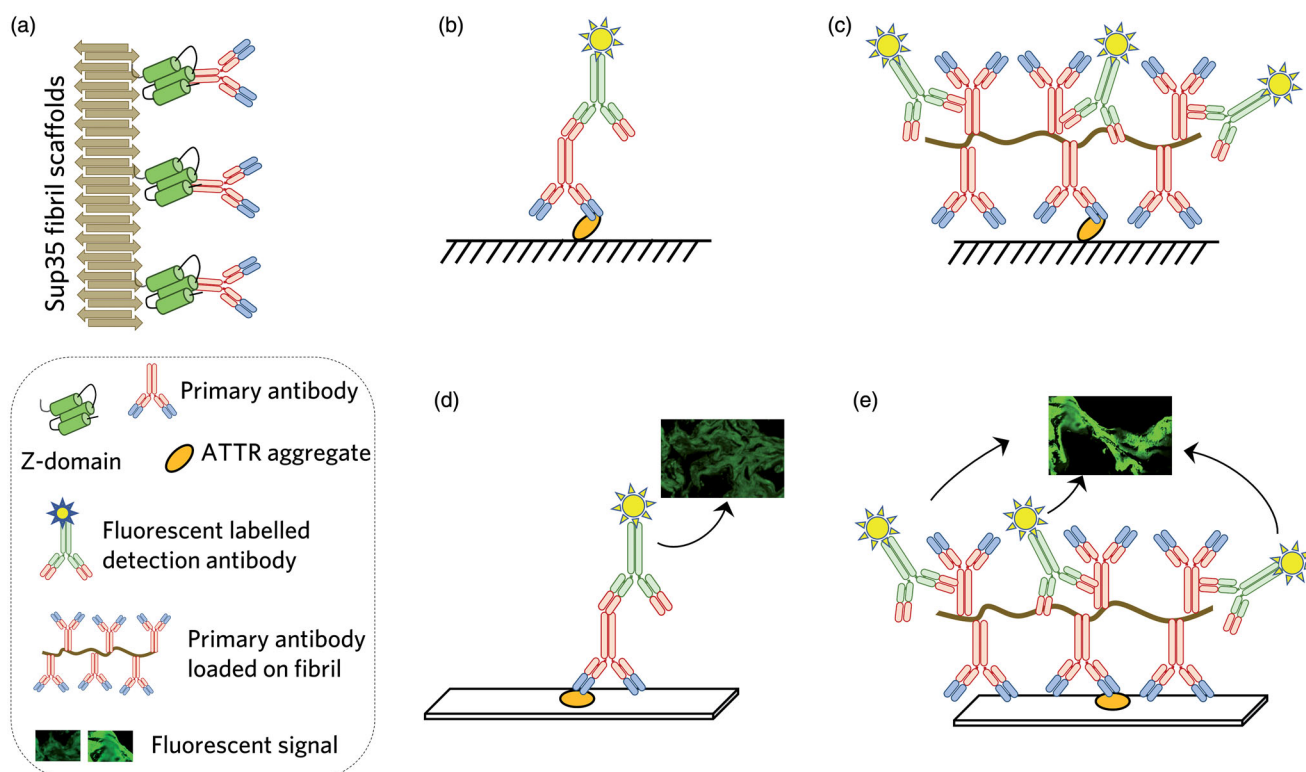


Figure 1. Illustration of the concepts for enhance detection of ATTR amyloid using a functional nanofibril-based assay. (a) The Ab-bNF are saturated with primary antibodies exploiting the ZZ domain on the fibril surface. (b) The conventional indirect immunoassay relies on a primary antibody against TTR, which is then detected by a fluorescent conjugated secondary antibody. (c) In the enhanced immunoassay, the Ab-bNF saturated with TTR-specific primary antibodies (TTR-bNF) bind the antigen and increase the number of secondary antibody binding sites per antigen. This strategy results in fluorescence signal enhancement. (d) ATTR amyloid-containing section is subjected to conventional immunofluorescence labelling and compared with (e) enhanced immunolabeling utilising TTR-bNF to obtain an enhanced signal.

Uppsala, Sweden) centrifuge using an F9-6 × 1000 LEX rotor. The cell pellet from 1 L culture was dissolved in 30 ml 25 mM Tris-HCl buffer containing one protease inhibitor tablet (Roche, Basel, Switzerland) and stored at −20 °C. Upon use, the cells were thawed and sonicated following a standard *E. coli* lysis procedure. Lysed cells were centrifuged at 17,000 rpm for 30 min at 4 °C using an F21-8x50y rotor in a Sorvall LYNX 6000 (Thermo Scientific) centrifuge. The supernatant was subjected to (NH₄)₂SO₄ precipitation (0–50% (NH₄)₂SO₄ cut), followed by another round of centrifugation. The supernatant was saved and filtered through 0.45 μm filter, and desalted by two rounds of overnight dialysis against 25 mM Tris-HCl using a 6–8 kDa dialysis membrane (Spectrum Labs, USA). The dialysed sample was concentrated using a Vivaspin 20 spin column (Sartorius, Germany) with a molecular mass cut-off of 5 kDa. The concentrated solution was loaded on a MonoQ 10/100 GL column (GE Healthcare, Uppsala, Sweden) equilibrated with 25 mM Tris HCl at pH 7.0 (buffer A), and bound proteins were eluted with buffer A containing 1 M NaCl. Purification was followed by size exclusion chromatography on a Superdex75 column (GE Healthcare) equilibrated with 50 mM Na-phosphate at pH 7.4 with 100 mM NaCl. The protein purity was confirmed by SDS-PAGE, and soluble M-TTR was snap-frozen and stored at −80 °C until use. The proteins Sup35(1-61) and Sup35(1-61)-ZZ were expressed and purified as described earlier [21].

Preparation of Ab-bNF

Soluble Sup35 (8 μg) diluted in fibrillation buffer (FB; 30 mM Tris pH 8.0, 200 mM NaCl) was sonicated in a Branson 2510 ultrasonication bath for eight minutes. This process produced fibrillar seeds (50 μL) that were immediately transferred to a sterile 1.5 ml Eppendorf vial containing soluble Sup35 (79 μg) and Sup35-ZZ (50 μg) in 220 μL FB. Fibrils were allowed to form for 30 min and then the reaction mixture was diluted by adding 100 μL FB, followed by 72 h incubation at room temperature (RT). The fibrils were pelleted by centrifugation at 5,000 × g using a Heraeus Pico 17 centrifuge (Thermo Scientific) for 10 min, and the supernatant was removed. The final molar ratio of Sup35 to Sup35-ZZ was 1:0.33.

Atomic force microscopy

The morphology of Ab-bNF was analysed using a Bruker Dimension FastScan Bio (Bruker, USA) atomic force microscope (AFM) equipped with a ScanAsyst Air probe. The Ab-bNF preparation (0.25 mg/mL) was diluted 10 times with deionised water, and approximately 6 μL were applied onto a freshly cleaved mica plate. The sample was allowed to dry overnight, and images of 1 μm × 1 μm or 2 μm × 2 μm were recorded by scanning at 1.99 Hz sample rate with 512 lines and 512 samples/lines.

Preparation of TTR-bNF

TTR isolated from a patient with ATTR amyloidosis was used for production of TTR (1899) antiserum in rabbit. Antiserum was added to Ab-bNF (binding capacity: 1.8 μg antibody/μg Ab-bNF) and incubated in 50 mM Tris pH 7.6, 150 mM NaCl (buffer T), at RT for 60 min. The complex (TTR-bNF = Ab-bNF and TTR antibody) was then pelleted at 5,000 × g using a Heraeus Pico 17 centrifuge (Thermo Scientific) for 10 min. The supernatant was removed, and the pellet was washed with buffer T and diluted in the same buffer.

TTR-bNF microplate immunoassay

M-TTR used as antigen was two-fold serial diluted from 1000 to 2.9 pg/mL in 0.1 M sodium carbonate-bicarbonate at pH 9.8 (coupling-buffer) and triplicate 100 μL/well portions were dispensed in a Greiner F-bottom black high-binding, 96-well plate (Sigma Aldrich). The antigen was allowed to bind overnight with gentle shaking at 4 °C. On the next day, non-bound TTR was removed, and unbound sites were blocked by 2% bovine serum albumin (BSA) in buffer T (300 μL/well) for 3 h at RT. The plate was then washed three times with buffer T containing 0.05% Tween 80 (buffer R), with 400 μL per well. The TTR-bNF complex was diluted in buffer T containing 0.75% BSA to 6.5 μg Ab-bNF and ≈11.7 μg primary antibody (1899), and 100 μL were added to each well. The plate was incubated at RT for 2.5 h, and then washed three times with buffer R, with 400 μL/well. Next, each well was incubated with 100 μL of goat anti-rabbit antibody conjugated with Alexa Fluor 488 (GAR-Alexa 488; Invitrogen, Carlsbad, CA), diluted 200 times in buffer T containing 0.75% BSA at RT for 1.5 h. Finally, the plate was washed five times with buffer R, and the fluorescence signal was measured at an excitation and emission wavelength of 485 and 520 nm, respectively, in a Polarstar Omega (BMG Labtech, Offenburg, Germany). As reference, conventional indirect immunoassay was performed using an identical set-up as in the TTR-bNF immunoassay, except that 10 μg/mL primary antibody (1899) diluted in buffer T was added to each well instead of the TTR-bNF. As blanks for both the conventional and TTR-bNF assay, the M-TTR concentration in the initial immobilisation step was 0 pg/mL. The blank samples were used to calculate the signal detection limit y_{dl} of the assay as:

$$y_{dl} = y_{blank} + 3s$$

where y_{blank} is the average value of seven blank measurements and s is the standard deviation [24].

Preparation of tissue section

Formalin-fixed paraffin-embedded heart tissue from two patients (Case 1 and Case 2) diagnosed with ATTR amyloidosis were used in the study. The amyloid protein isolated from both cases has been sequenced and confirmed to be of type A, consisting of C-terminal fragments and full-length

TTR [25]. Renal tissue from one patient diagnosed with AA amyloidosis of vascular type [26] were included and used for characterisation of TTR-bNF and AA-bNF binding *in situ*. The human material was obtained from the amyloid tissue bank and has been approved for research use by the Ethics Committee at Uppsala University. Sections, 6 μm thick, were placed on plus slides (VWR, Sweden) and heat-treated at 80 °C for 3 h. The sections were deparaffinized in xylene and rehydrated by incubation in decreasing ethanol concentrations, followed by rinsing in water and buffer T. A mouse was given a subcutaneous injection of 1% silver nitrate to stimulate SAA synthesis 24 h before sacrifice. After fixation in 10% neutral buffered formalin, the tissue was snap-frozen, and 10 μm thick sections were cut and dried onto plus slides. The sections were soaked in buffer T before incubation with Ab-bNF.

Immunofluorescence labelling

Ab-bNF (5 μg) containing 9 μg primary antibody or 7.5 μg Ab-bNF containing 13.5 μg primary antibody in buffer T was added to tissue sections. Overnight incubation took place in a humidity chamber at RT. The next day, the sections were rinsed four times in buffer T, followed by incubation with GAR-Alexa 488 or GAR-Alexa 647 (Invitrogen, Carlsbad, CA), diluted 1:1000 in buffer T at RT for 2 h. This was followed by rinsing four times in buffer T and then mounting with PBS-glycerol (1:1) containing 1 $\mu\text{g}/\text{mL}$ DAPI (Invitrogen, Carlsbad, CA). The sections were stored at 4 °C until analysis. For comparison, indirect immunolabeling with decreasing antibody concentrations of (1 μg , 0.5 μg , or 0.25 μg) was performed on sections from the same tissue. Detection, rinsing, and mounting was performed as for the enhanced assay.

Congo red staining

Deparaffinized and dehydrated sections were incubated with solution A containing 80% ethanol saturated with NaCl and 1% NaOH for 20 min, followed by incubation in solution B containing solution A saturated with Congo red and 1% NaOH for 20 min. After staining, the sections were rinsed in absolute ethanol and mounted with Mountex (HistoLab, Gothenburg, Sweden).

Microscopy

Immunolabeled tissue sections were analysed with a Zeiss LSM 780 confocal microscope (Carl Zeiss AG, Oberkochen, Germany). Images were acquired at 20 \times magnification. Congo red stained sections were analysed with an Olympus BX40 microscope fitted with polarisation filters (Olympus, Japan).

Results

TTR-bNF microplate immunoassay

AFM was used for analysing the morphology of Ab-bNF. The fibril lengths were determined to be within the range of 0.1–0.5 μm (Figure 2(a)). Some fibrils appeared as bundle-like assemblies (Figure 2(a), bottom), most likely due to amyloid fibrils' sticky nature. First, we sought to verify whether the TTR-bNF could be used to enhance the fluorescence signal in an indirect immunoassay, as outlined in Figure 1. In this assay, an engineered stable monomeric TTR variant was used as antigen. In the variant TTR, phenylalanine and leucine at positions 87 and 110 have been replaced with methionine. The mutations introduced into the subunit interfaces block tetramerization of M-TTR by steric clashing. M-TTR is a good mimic of wt-TTR and does not form amyloid fibrils unless partially denatured

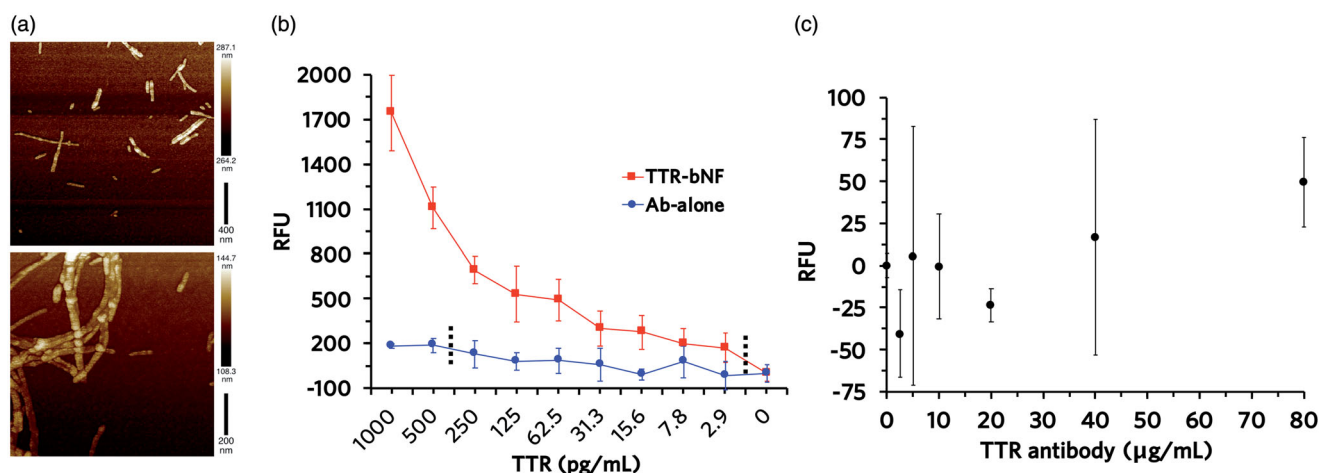


Figure 2. (a) AFM micrograph showing the short fibrils (top) and bundle-like morphologies (bottom) of Ab-bNF. The Ab-bNF was imaged by scanning areas with size 2 $\mu\text{m} \times 2 \mu\text{m}$ (top) and 1 $\mu\text{m} \times 1 \mu\text{m}$ (bottom) at 1.99 Hz sample rate with 512 lines and 512 samples/lines. (b) Comparison of the TTR-bNF-based assay (red) with the indirect immunoassay (blue). In the TTR-bNF-based assay, the Ab-bNF saturated with primary antibody served as the specific antigen recognition agent. The indirect immunoassay was performed identical to the TTR-bNF immunoassay, except that Ab-bNF was not included. The black dotted lines (---) represent the signal detection limit. (c) Plot showing that the fluorescence cannot be increased in an indirect immunoassay by increasing the antibody concentration without Ab-bNF. The background fluorescence corresponding to the primary antibody concentration was subtracted from each data point. The error bars in both (b) and (c) represent the standard deviation for $n = 3$ replicates.

[22]. By utilising the TTR-bNF, a 200-fold increase in assay sensitivity was measured, compared to a conventional indirect immunoassay (Figure 2(b)). This was determined by estimating the analyte concentration necessary to obtain significant fluorescence above the signal detection limit, which is the minimum detectable signal [24]. The signal detection limit was found to be below the lowest concentration tested in the TTR-bNF based assay, but was estimated to be 1.5 pg/mL. The signal detection limit for the reference assay was estimated to be 360 pg/mL. This level of detection is superior to that reported for previously developed protocols that utilise functional nanofibrils and display GFP on their surface [27–29].

To further assess whether the enhanced signal is Ab-bNF assisted or originates from the extra amount of antibody employed in the assay, we performed a control experiment in which 1000 pg/mL M-TTR, which was the highest concentration in the experimental assay, was immobilised in a 96-well plate. The conventional indirect immunoassay was then performed with an increasing concentration of primary antibodies. The results showed no linear dependency between the fluorescence signal and the primary antibody concentration (Figure 2(c)). Thus, we concluded that the amplified signal in our set-up is derived solely from the increased number of secondary antibodies that are recruited to the antigen *via* the Ab-bNF, as depicted in Figure 1.

TTR-bNF immunofluorescence labelling

Since our concept yielded promising results in the microplate format, we next examined whether Ab-bNF can be used to improve the sensitivity of an immunofluorescence assay. As with the microplate assay, we first compared the binding pattern of TTR-bNF and TTR primary antibody (1899) to TTR amyloid-containing tissue from Case 1. The indirect immunofluorescence labelling was carried out with 0.25 μ g, 0.5 μ g, and 1 μ g primary antibody per tissue section, followed by the addition of a fluorophore-conjugated secondary antibody. Strong fluorescence, indicating TTR amyloid presence, was observed in sections incubated with 0.25 μ g primary antibody, while the signal in sections incubated with 0.5 μ g and 1 μ g primary antibody appeared weaker (Figure 3(a–c)). The lower fluorescence signal observed in tissue sections incubated with higher antibody concentrations is likely due to steric hindrance [30,31].

For TTR-bNF immunofluorescence labelling, 9 μ g or 13.5 μ g primary antibody (*via* Ab-bNF) was added to each tissue section. As expected, the use of TTR-bNF yielded a strong fluorescence signal and all reactivity detected was strongly associated with amyloid deposits (Figure 3(d–e)). Interestingly, the fluorescent signal observed in tissue sections incubated with 13.5 μ g antibody bound to Ab-bNF was much stronger than that observed in sections incubated with 9 μ g antibody bound to Ab-bNF. This result confirms that the enhanced signals are TTR-bNF assisted. As mentioned previously, the detection sensitivity did not improve on increasing the concentration of primary antibody using indirect immunofluorescence labelling (Figure 3(a–c)). Using TTR-bNF, we successfully employed almost 10-fold

more primary antibody in the immunofluorescence labelling protocol, thereby achieving an enhanced signal.

However, it is well known that amyloid aggregates are sticky and tend to bind non-specifically to proteins and other cellular components [32–34]. Therefore, to exclude the possibility that the detected reactivity originates from unspecific binding, we included several negative controls. At first, TTR amyloid sections were incubated with empty Ab-bNF followed by incubation with secondary antibody to exclude unspecific interaction between the nanofibrils and the amyloid containing tissue (Figure 3(f)). Secondly, we tested for unspecific binding of the secondary antibody to the tissue structures by not including Ab-bNF and primary antibody in the labelling protocol (Figure 3(g)). To verify that TTR-bNF recognises TTR amyloid specifically and not amyloid aggregates in general, tissue sections containing AA amyloid were incubated with the TTR-bNF complex (Figure 3(h)). Furthermore, we examined whether signals could be detected after an irrelevant antibody was loaded onto the Ab-bNF. For this, an AA-specific primary antibody was used to produce AA-bNF and incubated with TTR amyloid containing section (Figure 3(i)). As expected, no amyloid reactivity appeared in any of these control experiments. In addition, we tested tissue autofluorescence by analysing TTR amyloid sections in the absence of Ab-bNF, or primary antibody, or secondary antibody (Figure 3(j)). The TTR section alone did not give rise to any fluorescent signal, excluding autofluorescence originating from the amyloid-containing tissues. From all these control experiments, it can be concluded that the TTR-bNF binds specifically to TTR amyloid. The specificity of the Ab-bNF, when loaded with a specific primary antibody towards the target antigen, was further illustrated by loading an anti-AA antibody on the Ab-bNF (AA-bNF), followed by incubation with AA amyloid sections. Exchanging the primary antibody and tissue section in the enhanced method also resulted in strong amyloid-specific reactivity (Figure 3(k)), which clearly demonstrates our method's versatility.

We also tested the ability of TTR-bNF and AA-bNF to bind to their native forms of TTR and SAA, respectively. Sections from mouse liver were used and TTR-bNF revealed almost no labelling with hepatocytes (results not shown), possibly depending on a limited TTR expression. The SAA expression is low in healthy individuals but expected to be high in the liver from an inflamed mouse. The AA-bNF labels the hepatocytes in these sections indicating that binding also occurs to the native protein (Figure 3(l)).

Next, employing TTR-bNF, we explored whether an enhanced signal can be achieved by immunofluorescence labelling of tissue sections that contain small amounts of amyloid. For this experiment, tissue from Case 2, which contained small ATTR deposits, were used (Figure 4(a)). The same experimental conditions and the same amount of primary antibody, i.e. 9 μ g or 13.5 μ g, as in the previous assay were used. This experiment demonstrated that the enhanced method has the potential to amplify amyloid-specific signals from minute amyloid deposits in tissue (Figure 4(b–c)). Furthermore, pathological amyloid deposits are

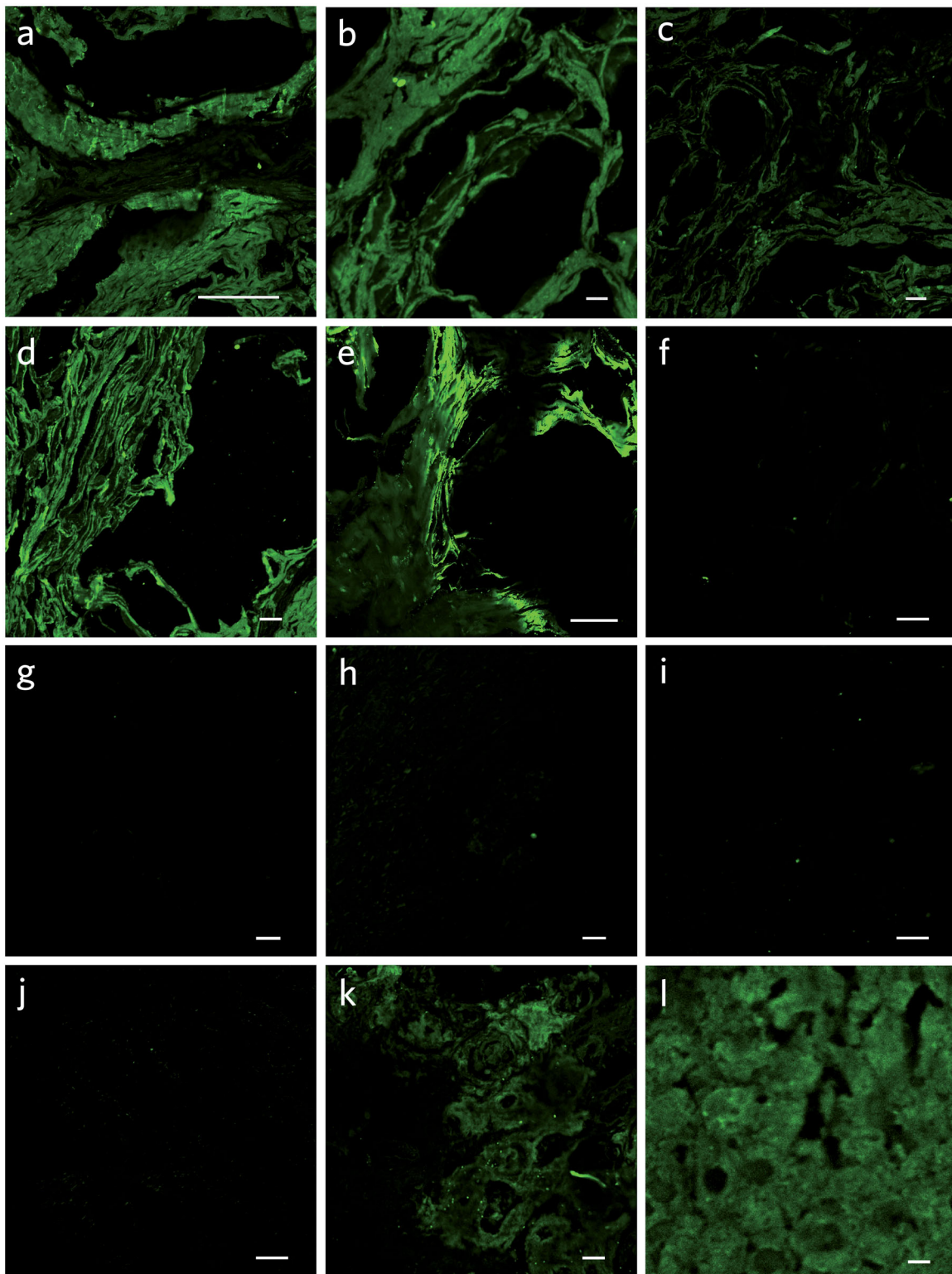


Figure 3. (a–c) Representative confocal images of indirect immunolabeling of *ex vivo* tissue from Case 1 using TTR-specific primary antibody alone. The antibody amount was 0.25 μg (a), 0.5 μg (b), or 1 μg (c). (d–e) Fluorescence from the enhanced immunolabeling assay in which the Ab-bNF were saturated with primary antibody before being applied onto the tissue sections. (d) 5 μg Ab-bNF:9 μg Ab. (e) 7.5 μg Ab-bNF:13 μg Ab. (f–j) Negative controls. (f) Ab-bNF (7.5 μg) without primary Ab was applied onto TTR amyloid sections. (g) Secondary Ab alone was added to TTR amyloid sections. (h) The TTR-bNF complex (7.5 μg Ab-bNF:13 μg Ab) was applied to AA amyloid sections. (i) TTR amyloid section incubated with AA-specific primary antibody on Ab-bNF (AA-bNF = 5 μg Ab-bNF:9 μg Ab). (j) TTR amyloid section in the absence of Ab-bNF, or primary Ab, or secondary Ab. (k) AA amyloid section incubated with AA-bNF (5 μg Ab-bNF:9 μg Ab), serving as another control to show the specificity of Ab-bNF. (l) mouse liver section incubated with AA-bNF (7.5 μg Ab-bNF:13 μg Ab). Images were captured at 20 \times magnification. The scale bar represents 200 μm .

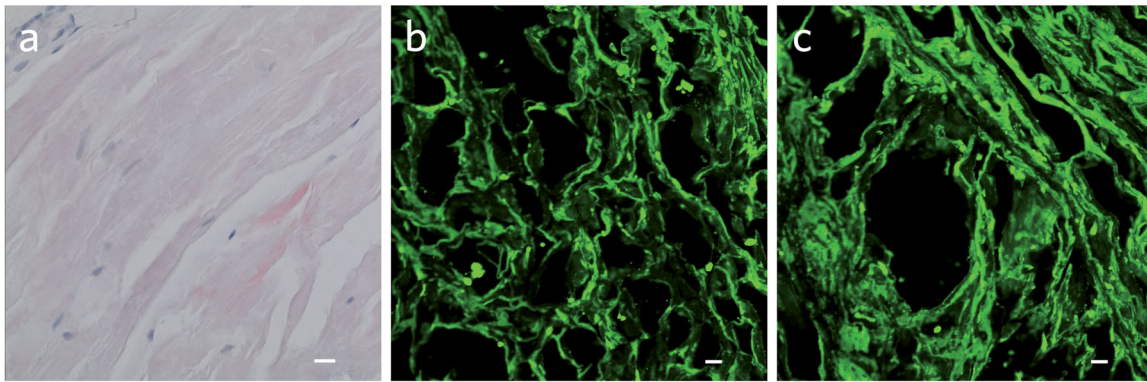


Figure 4. (a) *Ex vivo* tissue sections from Case 2 containing minute ATTR amyloid deposits, stained with Congo red. (b–c) Enhanced fluorescence signal from the same case using the TTR-bNF assay. The concentrations of the TTR-bNF complex are 5 µg Ab-bNF:9 µg Ab (b), and 7.5 µg Ab-bNF:13 µg Ab (c). The scale bar represents 200 µm.

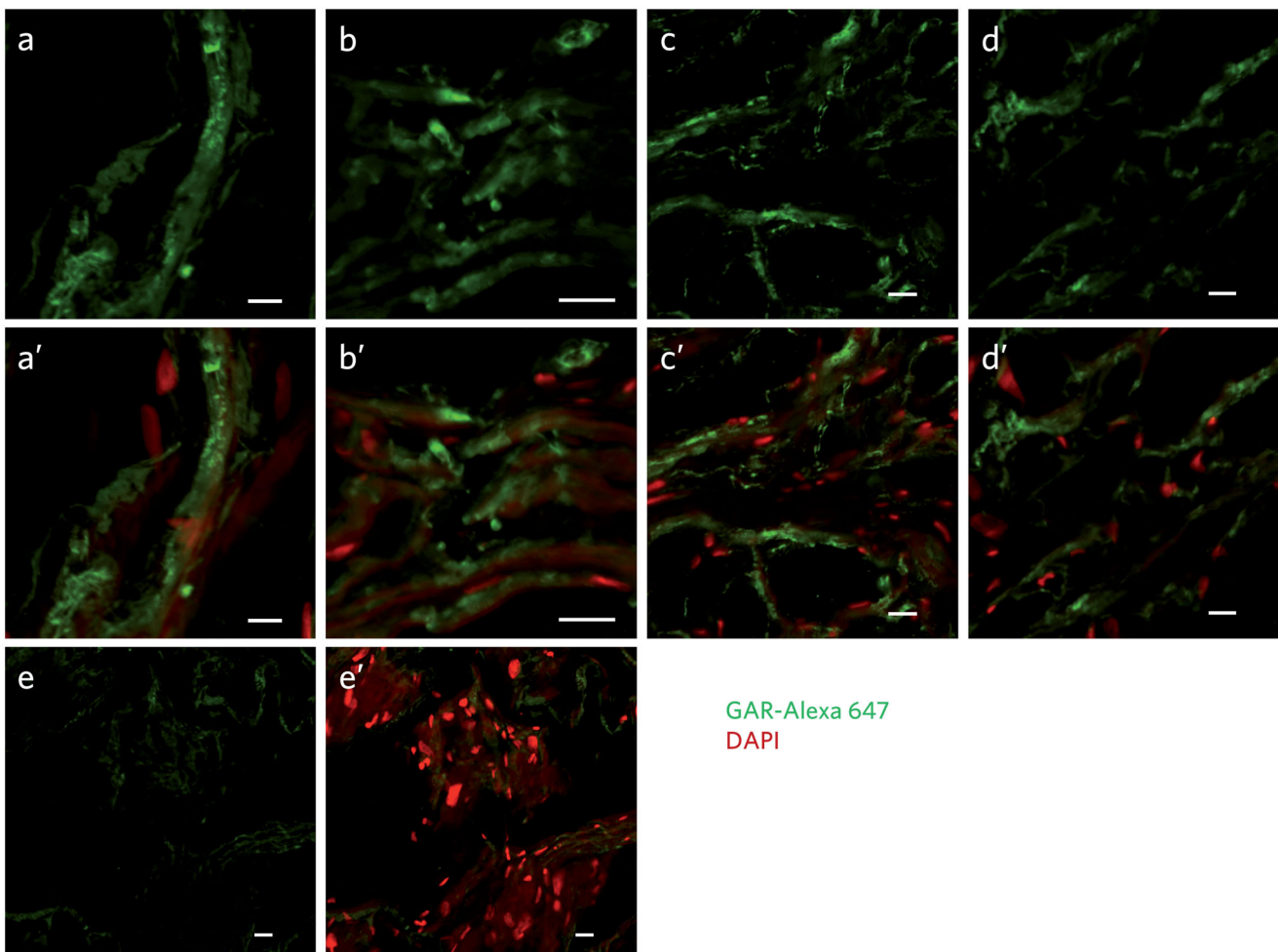


Figure 5. (a–d) Representative images of the enhanced fluorescence signal from Case 2 while using a diluted TTR-bNF complex. 7.5 µg Ab-bNF:13 µg Ab preparation was two-fold diluted to 3.75 µg Ab-bNF:6.5 µg Ab (a), 1.87 µg Ab-bNF:3.25 µg (b), 0.93 µg Ab-bNF:1.62 µg (c), and 0.47 µg Ab-bNF:0.84 µg (d), and applied onto the tissue sections. (a'–d') Composite images of (a–d). (e) A tissue section incubated with 1 µg antibody (approximately the same amount at the lowest concentration in the dilution of the TTR-bNF complex) without being loaded on Ab-bNF. (e') Composite image of (e). The scale bar represents 200 µm.

known to contain other cellular components as well as fibrillar proteins, together with the main protein precursor. It has previously been shown that apolipoprotein A-IV amyloid co-deposits with TTR in ATTR amyloidosis [35–37]. While detecting the presence of ATTR amyloid deposits in tissue with Congo red, signals from other amyloid deposits may contribute to the final signal, since Congo

red binds to the generic amyloid structure, i.e. β -pleated sheet configuration [38]. In contrast, the TTR-bNF assay contains an ATTR-specific antibody, which implies that the reactivity is exclusively from the ATTR aggregates.

Finally, we investigated whether enhanced signals can still be achieved while using a more diluted TTR-bNF complex, and whether the signals are correlated with the

concentration of the complex. For this, the highest concentration of the complex used in the previous assay (7.5 μg Ab-bNF and 13 μg Ab) was two-fold diluted in series to 0.47 μg Ab-bNF and 0.81 μg Ab. Representative images of immunolabeled sections using the diluted TTR-bNF are shown in [Figure 5](#). The images display strong and amyloid-specific fluorescence signals that are also well-correlated with the concentration of the complex. This result is in line with expectations from this experiment. The experiment also demonstrated that loading primary antibody in the amount used in the conventional assay (0.25–1 μg /per tissue section) on the Ab-bNF amplifies amyloid-specific signals and markedly amplifies signals from smaller aggregates. Furthermore, this experiment also indicates that even higher reactivity from smaller aggregates can be obtained if a larger amount of TTR-bNF complex is employed.

Discussion

Highly sensitive detection of pathological markers is essential for the identification of early stages of diseases, including amyloid disease. Existing methods considered useful for ultra-low detection are digital ELISA, immuno PCR (iPCR), and surface plasmon resonance (SPR) assays [39–41]. In digital ELISA, isolation of microbeads that capture proteins, which are enzyme-labeled into 50 fL reaction chambers, has lowered the detection limit below the fM range. iPCR is also a highly sensitive method, but this assay's shortcomings are the significantly longer detection time and the need for additional functionalization of the antibodies [42]. To avoid the additional labelling step, SPR is a well-studied method for highly sensitive detection of biomarkers [43]. However, these types of assays require sophisticated and expensive laboratory equipment and are not suited for the detection of amyloid in tissue sections.

In the present study, we developed a method that can easily be implemented into existing immunoassay formats and does not require any additional detection equipment. We recently assembled protein nanofibrils that can hold one order of magnitude more IgG than any other commercially available antibody-binding medium [21]. We speculated that the large surface area of these fibrils could be used to improve the sensitivity of an immunoassay dramatically [44]. We here functionalised these protein nanofibrils (Ab-bNF) with an antibody against TTR for enhanced ATTR amyloid detection in patients with ATTR amyloidosis. The rationale behind this work is that an enhanced signal can be achieved from extremely low antigen concentrations, i.e. aggregates, if an increased number of antibodies can be connected to the antigen, preventing steric hindrance. Using the functionalised nanofibril, i.e. Ab-bNF, whose surface displays the antibody-binding Z domain [21], we linked a higher number of primary antibodies to the antigen. This provided an increased number of binding sites for the secondary antibody resulting in signal amplification.

The microplate immunoassay results showed that the methodology yields the expected signal amplification. The method is robust and reproducible, but there are some

considerations. The first critical factor in this experimental set-up is the length of Ab-bNF, since it determines the number of primary antibodies introduced into the system. Theoretically, more fluorescence could be achieved from longer fibrils that provide more signal-generating secondary antibody-binding sites. However, longer fibrils are heavier and might be more susceptible to uncontrolled release from the surface due to shearing forces during the washing steps. According to this hypothesis, shorter fibrils would most likely be less susceptible to uncontrolled release. A second critical point is the length distribution of the fibrils. Shorter fibrils with a more uniform length distribution may be beneficial in ensuring that the fibrils are evenly distributed to the microplate wells, as an uneven distribution of fibrils could contribute to variation between data points and high standard deviation [29]. We achieved the best results with approximate fibril lengths in the range 0.1–0.5 μm . Short Ab-bNF fibrils were produced by diluting the reaction mixture after 30 min, which is the beginning (immediately after primary nucleation) of the fibril elongation phase. The rationale behind this protocol is that the addition of seeds created by sonication leads to a higher number of fibrils at the beginning of the aggregation reaction, and the subsequent addition of buffer to the reaction mixture decreases the concentration of the monomers, which limits fibril elongation. Even though this approach helped to produce short Ab-bNF fibrils, we could not completely avoid diversity in length and the formation of bundle-like morphology. Therefore, the protocol should be further optimised to produce short Ab-bNF fibrils with a more uniform length distribution.

Steric hindrance prevents the antibody from simultaneous binding to all epitopes on a polyvalent antigen, where binding epitopes are closely spaced on the surface [31]. Thus, the addition of excess antibody in an immunolabeling experiment does not improve the reactivity. For immunolabeling experiments, lower antibody concentration is often preferred. However, lower antibody concentration may generate very weak signals, especially when targeting small antigen deposits (aggregates). Therefore, linking an additional antibody to the antigen, by any means, could offer a valuable tool in immunolabeling experiments. With the use of Ab-bNF, we succeeded in introducing 10-times more primary antibody to amyloid deposits on tissue sections, which resulted in very strong signals, indicating that our concept nicely tackles the steric hindrance issue. Moreover, our enhanced method demonstrated the potential to amplify fluorescence signals from minute amyloid deposits in tissue.

Taken together, the results generated in this pilot study show that the enhanced method has the potential for detection of a small amount of ATTR aggregates in tissue. The set-up could also open a new avenue for the detection of small pathological deposits in tissue that occur in a broad range of human and animal diseases.

Acknowledgments

We thank Prof. P. Hammarström, Department of Physics, Chemistry and Biology at Linköping University, Sweden, for providing the TTR plasmid, and Prof. P. Westermark, Department of Immunology,

Genetics and Pathology at Uppsala University for providing rabbit anti-human ATTR polyclonal (1899) antibody and human tissue samples.

Disclosure statement

The authors declare no conflicts of interest.

Funding

This work was supported by a grant from the Swedish Research Council Formas [grant number: 9422015-945] to MS and TH, by Novo Nordisk [grant number: NNF 180c0034256] and by a grant from the Swedish Diabetes Foundation [grant number: DIA 2017-296] to GTW.

ORCID

M. Mahafuzur Rahman  <http://orcid.org/0000-0003-4247-7766>
 Benjamin Schmuck  <http://orcid.org/0000-0003-4021-6458>
 Henrik Hansson  <http://orcid.org/0000-0002-6003-2982>
 Torleif Härd  <http://orcid.org/0000-0001-9813-9913>
 Gunilla T. Westermark  <http://orcid.org/0000-0003-1151-9986>
 Mats Sandgren  <http://orcid.org/0000-0002-2358-4534>

References

- [1] Benson MD, Buxbaum JN, Eisenberg DS, et al. Amyloid nomenclature 2020: update and recommendations by the International Society of Amyloidosis (ISA) nomenclature committee. *Amyloid*. 2020;27(4):217–222.
- [2] Robbins J. Transthyretin from discovery to now. *Clin Chem Lab Med*. 2002;40(12):1183–1190.
- [3] Hamilton JA, Benson MD. Transthyretin: a review from a structural perspective. *Cell Mol Life Sci*. 2001;58(10):1491–1521.
- [4] Westermark P, Sletten K, Johansson B, et al. Fibril in senile systemic amyloidosis is derived from normal transthyretin. *Proc Natl Acad Sci U S A*. 1990;87(7):2843–2845.
- [5] Cornwell GG, 3rd, Sletten K, Johansson B, et al. Evidence that the amyloid fibril protein in senile systemic amyloidosis is derived from normal prealbumin. *Biochem Biophys Res Commun*. 1988;154(2):648–653.
- [6] Westermark GT, Fändrich M, Westermark P. AA amyloidosis: pathogenesis and targeted therapy. *Annu Rev Pathol*. 2015;10:321–344.
- [7] Blank N, Hegenbart U, Dietrich S, et al. Obesity is a significant susceptibility factor for idiopathic AA amyloidosis. *Amyloid*. 2018;25(1):37–45.
- [8] Suhr OB, Herlenius G, Friman S, et al. Liver transplantation for hereditary transthyretin amyloidosis. *Liver Transpl*. 2000;6(3):263–276.
- [9] Berk JL, Suhr OB, Obici L, et al. Repurposing diflunisal for familial amyloid polyneuropathy: a randomized clinical trial. *JAMA*. 2013;310(24):2658–2667.
- [10] Maurer MS, Schwartz JH, Gundapaneni B, et al. Tafamidis treatment for patients with transthyretin amyloid cardiomyopathy. *N Engl J Med*. 2018;379(11):1007–1016.
- [11] Adams D, Gonzalez-Duarte A, O’Riordan WD, et al. Patisiran, an RNAi therapeutic, for hereditary transthyretin amyloidosis. *N Engl J Med*. 2018;379(1):11–21.
- [12] Li T, Huang X, Cheng S, et al. Utility of abdominal skin plus subcutaneous fat and rectal mucosal biopsy in the diagnosis of AL amyloidosis with renal involvement. *PloS One*. 2017;12(9):e0185078.
- [13] Halloush RA, Lavrovskaya E, Mody DR, et al. Diagnosis and typing of systemic amyloidosis: the role of abdominal fat pad fine needle aspiration biopsy. *CytoJournal*. 2010;6:24.
- [14] Nilsson KP, Hammarstrom P, Ahlgren F, et al. Conjugated polyelectrolytes-conformation-sensitive optical probes for staining and characterization of amyloid deposits. *Chembiochem*. 2006;7(7):1096–1104.
- [15] Nilsson KP, Aslund A, Berg I, et al. Imaging distinct conformational states of amyloid-beta fibrils in Alzheimer’s disease using novel luminescent probes. *ACS Chem Biol*. 2007;2(8):553–560.
- [16] Klingstedt T, Aslund A, Simon RA, et al. Synthesis of a library of oligothiophenes and their utilization as fluorescent ligands for spectral assignment of protein aggregates. *Org Biomol Chem*. 2011;9(24):8356–8370.
- [17] Hahn K, Nilsson KPR, Hammarstrom P, et al. Establishing and validating the fluorescent amyloid ligand h-FTAA (heptamer formyl thiophene acetic acid) to identify transthyretin amyloid deposits in carpal tunnel syndrome. *Amyloid*. 2017;24(2):78–86.
- [18] Sjolander D, Rocken C, Westermark P, et al. Establishing the fluorescent amyloid ligand h-FTAA for studying human tissues with systemic and localized amyloid. *Amyloid*. 2016;23(2):98–108.
- [19] Sjölander D, Bijzet J, Hazenberg BP, et al. Sensitive and rapid assessment of amyloid by oligothiophene fluorescence in subcutaneous fat tissue. *Amyloid*. 2015;22(1):19–25.
- [20] Eisele YS, Monteiro C, Fearn C, et al. Targeting protein aggregation for the treatment of degenerative diseases. *Nat Rev Drug Discov*. 2015;14(11):759–780.
- [21] Schmuck B, Sandgren M, Hard T. A fine-tuned composition of protein nanofibrils yields an upgraded functionality of displayed antibody binding domains. *Biotechnology J*. 2017;12(6):1–13.
- [22] Jiang X, Smith CS, Petrassi HM, et al. An engineered transthyretin monomer that is nonamyloidogenic, unless it is partially denatured. *Biochemistry*. 2001;40(38):11442–11452.
- [23] Groenning M, Campos RI, Fagerberg C, et al. Thermodynamic stability and denaturation kinetics of a benign natural transthyretin mutant identified in a Danish kindred. *Amyloid*. 2011;18(2):35–46.
- [24] Harris DC. Quantitative chemical analysis. 8th ed. New York City, NY: W. H. Freeman and Company; 2010. p. 103–104.
- [25] Bergstrom J, Gustavsson A, Hellman U, et al. Amyloid deposits in transthyretin-derived amyloidosis: cleaved transthyretin is associated with distinct amyloid morphology. *J Pathol*. 2005;206(2):224–232.
- [26] Westermark GT, Sletten K, Westermark P. Massive vascular AA-amyloidosis: a histologically and biochemically distinctive subtype of reactive systemic amyloidosis. *Scand J Immunol*. 1989;30(5):605–613.
- [27] Men D, Zhou J, Li W, et al. Fluorescent protein nanowire-mediated protein microarrays for multiplexed and highly sensitive pathogen detection. *ACS Appl Mater Interfaces*. 2016;8(27):17472–17477.
- [28] Men D, Zhang ZP, Guo YC, et al. An auto-biotinylated bifunctional protein nanowire for ultra-sensitive molecular biosensing. *Biosens Bioelectron*. 2010;26(4):1137–1141.
- [29] Men D, Guo YC, Zhang ZP, et al. Seeding-induced self-assembling protein nanowires dramatically increase the sensitivity of Immunoassays. *Nano Lett*. 2009;9(6):2246–2250.
- [30] Kent SP, Ryan KH, Siegel AL. Steric hindrance as a factor in the reaction of labeled antibody with cell surface antigenic determinants. *J Histochem Cytochem*. 1978;26(8):618–621.
- [31] Cowan R, Underwood PA. Steric effects in antibody reactions with polyvalent antigen. *J Theor Biol*. 1988;132(3):319–335.
- [32] Stefani M, Rigacci S. Protein folding and aggregation into amyloid: the interference by natural phenolic compounds. *Int J Mol Sci*. 2013;14(6):12411–12457.

- [33] Rahman MM, Zetterberg H, Lendel C, et al. Binding of human proteins to amyloid- β protofibrils. *ACS Chem Biol.* 2015;10(3):766–774.
- [34] Rahman MM, Westermark GT, Zetterberg H, et al. Protofibrillar and fibrillar amyloid- β binding proteins in cerebrospinal fluid. *J Alzheimers Dis.* 2018;66(3):1053–1064.
- [35] Benson MD, Buxbaum JN, Eisenberg DS, et al. Amyloid nomenclature 2018: recommendations by the International Society of Amyloidosis (ISA) nomenclature committee. *Amyloid.* 2018;25(4):215–219.
- [36] Bergstrom J, Murphy C, Eulitz M, et al. Codeposition of apolipoprotein A-IV and transthyretin in senile systemic (ATTR) amyloidosis. *Biochem Biophys Res Commun.* 2001;285(4):903–908.
- [37] Bergstrom J, Murphy CL, Weiss DT, et al. Two different types of amyloid deposits-apolipoprotein A-IV and transthyretin-in a patient with systemic amyloidosis. *Lab Invest.* 2004;84(8):981–988.
- [38] Yakupova EL, Bobyleva LG, Vikhlyantsev IM, et al. Congo Red and amyloids: history and relationship. *Biosci Rep.* 2019;39(1):BSR20181415.
- [39] Barletta JM, Edelman DC, Highsmith WE, et al. Detection of ultra-low levels of pathologic prion protein in scrapie infected hamster brain homogenates using real-time immuno-PCR. *J Virol Methods.* 2005;127(2):154–164.
- [40] Lubelli C, Chatgililoglu A, Bolognesi A, et al. Detection of ricin and other ribosome-inactivating proteins by an immuno-polymerase chain reaction assay. *Anal Biochem.* 2006;355(1):102–109.
- [41] Rissin DM, Kan CW, Campbell TG, et al. Single-molecule enzyme-linked immunosorbent assay detects serum proteins at subfemtomolar concentrations. *Nat Biotechnol.* 2010;28(6):595–599.
- [42] Chang L, Li J, Wang L. Immuno-PCR: an ultrasensitive immunoassay for biomolecular detection. *Anal Chim Acta.* 2016;910:12–24.
- [43] Martinez-Perdiguero J, Retolaza A, Bujanda L, et al. Surface plasmon resonance immunoassay for the detection of the TNF α biomarker in human serum. *Talanta.* 2014;119:492–497.
- [44] Castanheira AP, Barbosa AI, Edwards AD, et al. Multiplexed femtomolar quantitation of human cytokines in a fluoropolymer microcapillary film. *Analyst.* 2015;140(16):5609–5618.